

Principal Spine Shape Deformation Modes Using Riemannian Geometry and Articulated Models

Jonathan Boisvert^{1,2,3}, Xavier Pennec², Hubert Labelle³,
Farida Cheriet^{1,3}, and Nicholas Ayache²

¹ École Polytechnique de Montréal

P.O. Box 6079, Station Centre-Ville, Montréal H3C 3A7, Canada

jonathan.boisvert@polymtl.ca

² INRIA, Asclepius Project Team - 2004 route des Lucioles - BP 93
06902 Sophia Antipolis Cedex, France

³ Sainte-Justine Hospital, 3175, Chemin de la Côte-Ste-Catherine, Montréal, Canada

Abstract. We present a method to extract principal deformation modes from a set of articulated models describing the human spine. The spine was expressed as a set of rigid transforms that superpose local coordinates systems of neighbouring vertebrae. To take into account the fact that rigid transforms belong to a Riemannian manifold, the Fréchet mean and a generalized covariance computed in the exponential chart of the Fréchet mean were used to construct a statistical shape model. The principal deformation modes were then extracted by performing a principal component analysis (PCA) on the generalized covariance matrix. Principal deformations modes were computed for a large database of untreated scoliotic patients and the obtained results indicate that combining rotation and translation into a unified framework leads to an effective and meaningful method of dimensionality reduction for articulated anatomical structures. The computed deformation modes also revealed clinically relevant information. For instance, the first mode of deformation appeared to be associated with patients' growth, the second is a double thoraco-lumbar curve and the third is a thoracic curve.

1 Introduction

Most of the statistical shapes models currently used to describe anatomical structures are based on point to point correspondences extracted from images ([1,2] for example). However, points are not always the best choice of primitives. To deal with articulated anatomical structures a more natural choice would be to use frames (points associated with three orthogonal axes). The main reason for this choice is that frames enable a more natural analysis of the relative orientations and positions of the models.

The spine is one of the anatomical structures that is better described using frames instead of points. In this context, a frame is associated to each vertebra and the deformations of the spine are then described in terms of rigid transforms applied to those frames.

However, conventional statistical methods usually apply only in vector spaces, while rigid transforms naturally belong to a Lie group. Therefore, concepts as

simple as the mean and the covariance had to be generalized because addition and scalar multiplication are not defined in Lie groups. Probability and statistics applied to Riemannian manifolds [3] offer an elegant way to deal with those difficulties and variability models based on Lie groups can now be built. The Riemannian framework was also used in the context of statistical shape modelling to perform PGA (principal geodesic analysis) on medial axis representations (m-reps) [4].

Thus, it is now possible to compute a variability model of the spine based on the tools from the Riemannian geometry [5]. But a rigid transform has 6 DOF (degrees of freedom) and there are 5 lumbar and 12 thoracic vertebrae for a total of 102 DOF (excluding cervical vertebrae). The analysis of such large variability model can hardly be performed by a clinician. It is therefore necessary to find a way to reduce the dimensionality of the variability model and to extract only the most meaningful modes of variability.

Dimensionality reduction applied to the spine or to articulated models is not a new idea and methods were proposed in the past. As a part of a method that aim to predict the geometry of the spine based on the geometry of the trunk, Bergeron et al. [6] performed a principal component analysis on the 3D coordinates of vertebrae's center in the frequency domain. Principal components analysis was also used to process articulated body models (see, for instance, Gonzalez et al. [7] and Jiang and Motiai [8]). In that context, classical PCA was used on a representation that was either only based on 3D coordinates or only based on an angular description of the articulated body. However, using both positions and orientations would allow a better separation of different physiological phenomena such as pathological deformations and normal growth.

The main contributions of this paper will therefore be to propose a method based on Riemannian geometry to perform principal components analysis on an articulated model of the spine and to apply that method to a large database of scoliotic patients in order to construct the first statistical atlas of 3D deformation patterns for idiopathic scoliosis (a pathology that causes spine deformations).

2 Material and Methods

This section will be divided into four subsections. Firstly, elements of probability and statistics on Riemannian manifolds will be introduced. Secondly, a generalization of principal component analysis on Riemannian manifolds will be described. Then, the specialization of this method for articulated models will be tackled in the third subsection. Finally, the fourth subsection will explain how the extraction of articulated models is performed from spine radiographs.

2.1 Elements of Probability and Statistics on Riemannian Manifolds

Because there is no addition or scalar multiplication operations readily defined on rigid transforms, we need a way to generalize the notions of mean and directional dispersion. The distance is a general concept that can be used to perform those

generalisations and Riemannian geometry offers a mathematical framework to work with primitives when only a distance function is available.

In a complete Riemannian manifold \mathcal{M} the smallest smooth curve $\gamma(t)$ such that $\gamma(0) = x$ and $\gamma(1) = y$ is called a geodesic and the length of that curve is the distance between x and y . Two important maps can be defined from the geodesics: the exponential map Exp_x which maps a vector ∂_x of the tangent plane $T_x\mathcal{M}$ to the element reached in a unit time by the geodesic that starts at x with an initial tangent vector ∂_x and the logarithmic map Log_x which is the inverse function of Exp_x . In other words, these two maps enable us to “unfold” the manifold on the tangent plane (which is a vector space) and to project an element of the tangent plane to the manifold.

With the knowledge of Exp_x and Log_x , it is possible to compute the generalisations of the conventional mean and covariance. The following subsections will introduce those generalisations in the univariate and multivariate cases.

Fréchet Mean. For a given distance, the generalization of the usual mean can be obtained by defining the mean as the element μ of a manifold \mathcal{M} that minimizes the sum of the distances with a set of elements $x_{0\dots N}$ of the same manifold \mathcal{M} :

$$\mu = \arg \min_{x \in \mathcal{M}} \sum_{i=0}^N d(x, x_i)^2$$

This generalization of the mean is called the Fréchet mean. Since it is defined using a minimization, it is difficult to compute it directly from the definition. However, it can be computed using a gradient descent performed on the summation. The following recurrent equation summarizes this operation:

$$\mu_{n+1} = \text{Exp}_{\mu_n} \left(\frac{1}{N} \sum_{i=0}^N \text{Log}_{\mu_n}(x_i) \right) \quad (1)$$

Generalized Covariance. The variance (as it is usually defined on real vector spaces) is the expectation of the L_2 norm of the difference between the mean and the measures. An intuitive generalization of the variance on Riemannian manifolds is thus given by the expectation of a squared distance:

$$\sigma^2 = \frac{1}{N} \sum_{i=0}^N d(\mu, x_i)^2 \quad (2)$$

To create statistical shape models it is necessary to have a directional dispersion measure since the anatomical variability of the spine is anisotropic [5]. The covariance is usually defined as the expectation of the matricial product of the vectors from the mean to the elements on which the covariance is computed. Thus, a similar definition for Riemannian manifolds would be to compute the expectation in the tangent plane of the mean using the log map:

$$\Sigma = \frac{1}{N} \sum_{i=0}^N \text{Log}_{\mu}(x) \text{Log}_{\mu}(x)^T \quad (3)$$

Multivariate Case. The Fréchet mean and the generalized covariance make it possible to study the centrality and dispersion of one primitive belonging to a Riemannian manifold. However, to build complete statistical shape models, it would be most desirable to study multiple primitives altogether. Therefore, a generalized cross-covariance Σ_{fg} is needed.

$$\Sigma_{fg} = \frac{1}{N} \sum_{i=0}^N \text{Log}_{\mu_f}(f_i) \text{Log}_{\mu_g}(g_i)^T$$

A natural extension is to create a multivariate vector $f = [f_1, f_2, f_3, \dots, f_k]^T$ where each element corresponds to a part of a model made of several primitives. The mean and the covariance of this multivariate vector will thus be:

$$\mu = \begin{bmatrix} \mu_1 \\ \mu_2 \\ \vdots \\ \mu_k \end{bmatrix} \quad \text{and} \quad \Sigma = \begin{bmatrix} \Sigma_{f_1 f_1} & \Sigma_{f_1 f_2} & \dots & \Sigma_{f_1 f_k} \\ \Sigma_{f_2 f_1} & \Sigma_{f_2 f_2} & \dots & \Sigma_{f_2 f_k} \\ \vdots & \vdots & & \vdots \\ \Sigma_{f_k f_1} & \Sigma_{f_k f_2} & \dots & \Sigma_{f_k f_k} \end{bmatrix} \tag{4}$$

This is very similar to the conventional multivariate mean and covariance except that the Fréchet mean and the generalized cross-covariance are used in the computations.

2.2 Extraction of the Principal Deformations

The equation 4 allows us to compute a statistical shape model for a group of models made of several primitives. However, the different primitives will most likely be correlated which makes the variability analysis very difficult. Furthermore, the dimensionality of the model is also a concern and we would like to select only a few important uncorrelated components.

Unlike the manifold itself, the tangent plane is a vector space and its basis could be changed using a simple linear transformation. Thus, we seek an orthonormal matrix A ($AA^T = I$) to linearly transform the tangent plane ($\text{Log}_{\mu}(g) = A \text{Log}_{\mu}(f)$) such as the generalized covariance in the transformed tangent space is a diagonal matrix ($\Sigma_{gg} = \text{diag}(\lambda_1, \lambda_2, \dots, \lambda_k)$). The covariances of the transformed tangent space and of the original tangent space are connected by the following equation:

$$\Sigma_{gg} = \text{diag}(\lambda_1, \lambda_2, \dots, \lambda_k) = A \Sigma_{ff} A^T$$

If A is rewritten as $A = [a_1, a_2, \dots, a_k]^T$, then it is easy to show that:

$$[\lambda_1 a_1, \lambda_2 a_2, \dots, \lambda_k a_k] = [\Sigma_{ff} a_1, \Sigma_{ff} a_2, \dots, \Sigma_{ff} a_k] \tag{5}$$

The line vectors of the matrix A are therefore the eigenvectors of the original covariance matrix and the elements of the covariance matrix in the transformed space are the eigenvalues of the original covariance. This is the exact same procedure that is used to perform PCA in real vector spaces. Like for real vector

spaces, the variance is left unchanged since $\sigma^2 = \text{Tr}(\Sigma_{ff}) = \text{Tr}(\Sigma_{gg})$ and the cumulative fraction of the variance explained by the first n components is:

$$p = \frac{1}{\sigma^2} \sum_{i=1 \dots n} \lambda_i$$

A shape model can be re-created from coordinates of the transformed tangent space simply by going back to the original tangent space and projecting the model on the manifold using the exponential map. So if α_i is the coordinate associated with the i^{th} principal component, the following equation can be used to re-create a shape model:

$$S = \text{Exp}_\mu \left(\sum_{i=1}^k \alpha_i a_i \right)$$

2.3 Application to Articulated Models of the Spine

In this paper, the spine is modelled as a set of frames associated to local coordinates systems of vertebrae. The modifications of the spine geometry are thus modelled as rigid transforms that are applied to those frames. In order to compute the principal deformations modes (from equation 5), the exponential and logarithmic maps associated with a distance function on rigid transforms are needed.

A rigid transform is the combination of a rotation and a translation. Defining a suitable distance on the translational part is not difficult since 3D translations belong to a real vector space. However, the choice of a distance function between rotations is more complex.

To define a suitable distance function between rigid transforms, another representation of the rotations called the rotation vector is needed. This representation is based on the fact that a 3D rotation can be fully described by an axis of rotation supported by a unit vector n and an angle of rotation θ (see figure 1). The rotation vector r is then defined as the product of n and θ .

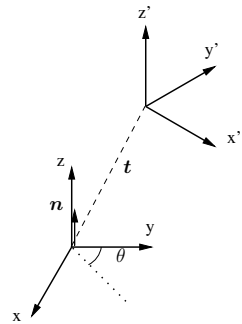


Fig. 1. Rigid transform expressed by an axis of rotation n , an angle of rotation θ and a translation vector t

The conversion from the rotation vector to the rotation matrix is performed using the Rodrigues equation:

$$R = I + \sin(\theta) \cdot S(n) + (1 - \cos(\theta)) \cdot S(n)^2 \quad \text{with} \quad S(n) = \begin{bmatrix} 0 & -n_z & n_y \\ n_z & 0 & n_x \\ -n_y & n_x & 0 \end{bmatrix}$$

And the inverse map (from a rotation matrix to a rotation vector) is given by the following equations:

$$\theta = \arccos\left(\frac{\text{Tr}(R) - 1}{2}\right) \quad \text{and} \quad S(n) = \frac{R - R^T}{2 \sin(\theta)} \tag{6}$$

Using the rotation vector representation, a left-invariant distance ($d(T_3 \circ T_1, T_3 \circ T_2) = d(T_1, T_2)$) between two rigid transformations can easily be defined:

$$d(T_1, T_2) = N_\omega(T_2^{-1} \circ T_1) \quad \text{with} \quad N_\omega(T)^2 = N_\omega(\{r, t\})^2 = \|r\|^2 + \|\omega t\|^2 \quad (7)$$

Where ω is used to weight the relative effect of rotation and translation, r is the rotation vector and t the translation vector. Because the selected distance function is left-invariant, we have $\text{Exp}_\mu(T) = \text{Exp}_{Id}(\mu^{-1} \circ T)$ and $\text{Log}_\mu(T) = \text{Log}_{Id}(\mu^{-1} \circ T)$. Furthermore, it can be demonstrated that the exponential and log map associated with the distance of equation 7 are the mappings (up to a scale) between the combination of the translation vector and rotation vector and the combination of the rotation matrix and the translation vector [9].

$$\text{Exp}_{Id}(T) = \begin{bmatrix} R(r) \\ \omega^{-1}t \end{bmatrix} \quad \text{and} \quad \text{Log}_{Id}(T) = \begin{bmatrix} r(R) \\ \omega t \end{bmatrix}$$

2.4 Extraction of Articulated Model of the Spine from Radiographs

The 3D geometry of the spine is digitized using a posterior-anterior and a lateral radiograph. Radiographs are used because it allows the patients to stand up during the acquisition (which is important since a large proportion of the spine deformation is hidden when patients lie down). Six anatomical landmarks are identified on the two radiographs. The 3D coordinates of the landmarks are computed using a triangulation algorithm and the deformation of a high-resolution template using dual kriging yields 16 additional reconstructed landmarks. The accuracy of this method was previously established to 2.6mm [10].

Once the landmarks are reconstructed in 3D, each vertebra is rigidly registered to its first upper neighbour and the resulting rigid transforms are recorded. By doing so, the spine is represented by a set of rigid transforms (see the figure 2). This set of inter-vertebral transforms will be used to compute the mean and covariance of the spine shape.

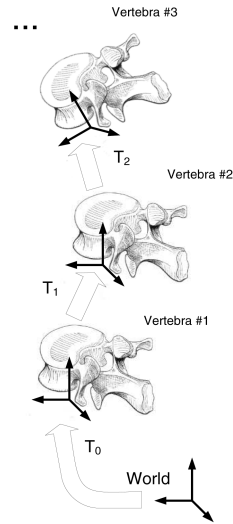


Fig. 2. Frames and transforms used to express the spine as an articulated model

3 Results and Discussion

The method described in the previous sections was applied to a group of 307 scoliotic patients. The patients selected for this study had not been treated with

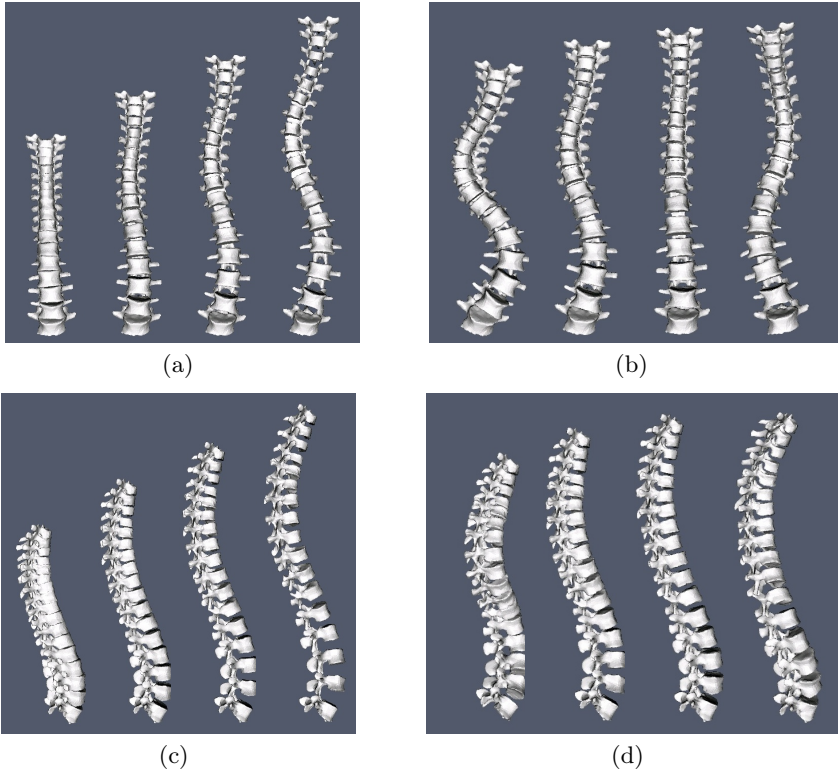


Fig. 3. First principal deformation mode (reconstructions for $-3\sqrt{\lambda_1}$, $-\sqrt{\lambda_1}$, $\sqrt{\lambda_1}$, $3\sqrt{\lambda_1}$), posterior-anterior view (a) and lateral view (c). Second principal deformation mode (reconstructions for $-3\sqrt{\lambda_2}$, $-\sqrt{\lambda_2}$, $\sqrt{\lambda_2}$, $3\sqrt{\lambda_2}$), posterior-anterior view (b) and lateral view (d).

any kind of orthopaedic treatment when radiographs were taken. Therefore, the inter-patients variability observed was mainly caused by anatomical differences and not by any treatments. The ω constant was set to 0.05 because this value leads to approximatively equal contributions of the rotation and the translation to the variance.

To illustrate the different deformation modes retrieved using the proposed method, four models were reconstructed for each of the first four principal deformation modes. Those models were reconstructed by setting α_k to $-3\sqrt{\lambda_k}$, $-\sqrt{\lambda_k}$, $\sqrt{\lambda_k}$ and $3\sqrt{\lambda_k}$ for $k = 1 \dots 4$ while all others components (α_i with $i \neq k$) were set to zero (see figures 3 and 4).

A visual inspection reveals that the first four principal deformation modes have clinical meanings. The first appears to be associated with the patient growth because it is mainly characterized by an elongation of the spine and also includes a mild thoracic curve. The second principal deformation mode could be described as a double thoraco-lumbar curve, because there are two curves: one in the thoracic segment (upper spine) and another in the lumbar segment (lower spine).

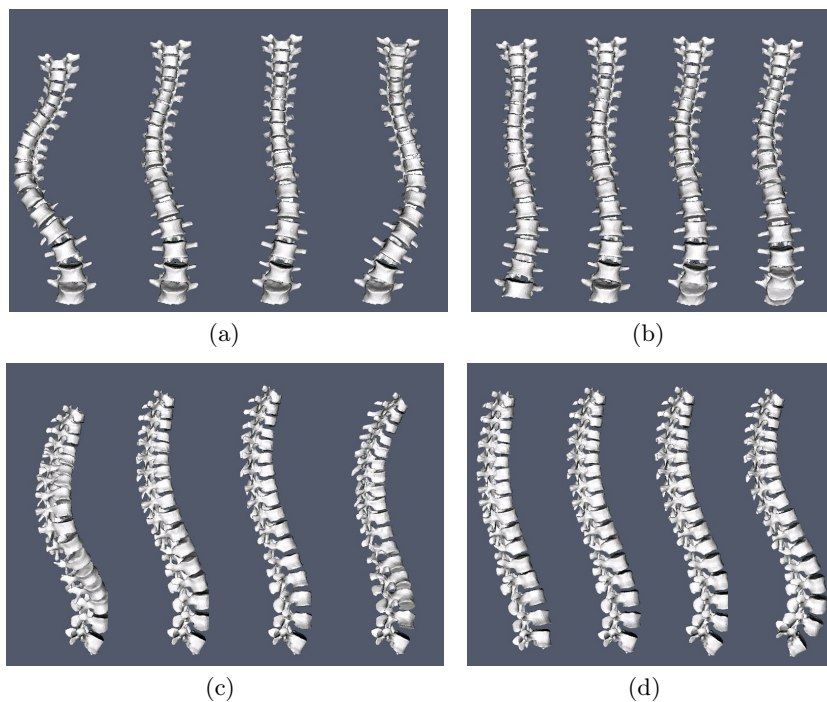


Fig. 4. Third principal deformation mode (reconstructions for $-3\sqrt{\lambda_3}$, $-\sqrt{\lambda_3}$, $\sqrt{\lambda_3}$, $3\sqrt{\lambda_3}$), posterior-anterior view (a) and lateral view (c). Fourth principal deformation mode (reconstructions for $-3\sqrt{\lambda_4}$, $-\sqrt{\lambda_4}$, $\sqrt{\lambda_4}$, $3\sqrt{\lambda_4}$), posterior-anterior view (b) and lateral view (d).

The third principal mode of deformation is a simple thoracic curve (the apex of the curve is in the thoracic spine), but it is longer than the thoracic curve observed in the first principal component. It is also interesting to note that, in addition to the curves visible on the posterior-anterior view, the second and third principal deformation modes are also associated with the development of a kyphosis (back hump) on the lateral view. Finally, the fourth component is a lumbar lordosis (lateral curve of the lumbar spine).

Those curve patterns are routinely used in different clinical classifications of scoliosis (used to plan surgeries). For instance, the reconstructions built from the first principal deformation mode would be classified using King's classification [11] as a type II or III (depending on which reconstruction is evaluated), the second deformation mode would be associated to King's type I or III and the third principal deformation could be associated to King's type IV.

Previously those patterns were derived from surgeons' intuition using 2D images and clinical indices, whereas it is now possible to automatically compute those patterns from statistics based only on 3D geometries. This also makes it possible, for example, to compare principal deformation modes of different subgroups of scoliotic patients.

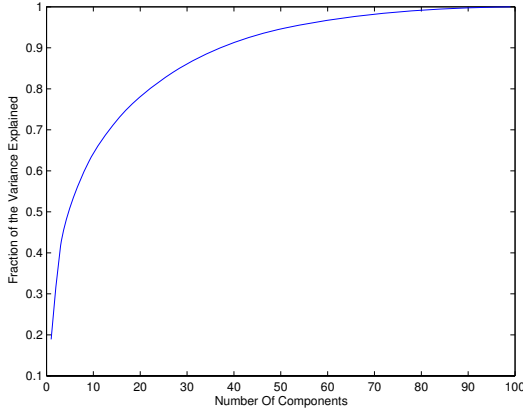


Fig. 5. Fraction of the variance explained by the n^{th} most important principal deformation modes

Furthermore, the cumulative variance explained by an increasing number of principal deformations modes (illustrated at figure 5) shows the capacity of the proposed method to reduce the dimensionality of the model while keeping a large part of the original variance.

Finally, the algorithm is not very sensitive to the exact value of ω (values between 0.01 and 0.25 were tried and yielded similar results with our database), but setting a value considerably too high or too low would discard either the rotation or translation part of the rigid transforms from the analysis.

4 Conclusion

A method to extract the principal modes of deformation from articulated models was described. The method consists in performing a principal component analysis in the tangent space of a Riemannian manifold (the Lie group of rigid transforms equipped with a metric). We applied this method to a database of scoliotic patients reconstructed in 3D using stereo radiographs. Clinically relevant patterns of deformations were extracted from that database and dimensionality reduction was successfully achieved. Results also suggest that PCA applied to a suitable representation of the spine, namely a set of rigid transforms, leads to an algorithm that can expose natural modes of deformation of the spine. However, it might be interesting to validate the method using an high accuracy imaging apparatus and a deformable spine phantom.

One of the reasons to perform dimensionality reduction on statistical shape models is to reduce the number of DOF that needs to be optimized during model registration. The proposed method will therefore be integrated to a spine registration algorithm in the future. It might also be useful for the integration

of a large number of rigid structures in non-rigid registration procedures [12] of the whole human torso.

Also, the current method takes only into account the shape of the spine and not the shape of the individual vertebrae. But the deformations of individual vertebrae are connected to the deformations of the whole spine (see, for example, the vicious cycle described by Stokes et al. [13]). Thus, future developments might include the construction of hybrid models where the global shape of the spine would be modelled using inter-vertebral rigid transforms and the shape of individual vertebrae would be taken into account using spherical harmonics or medial axis representations (for instance).

References

1. Lorenz, C., Krahnstover, N.: Generation of point-based 3d statistical shape models for anatomical objects. *Comput. Vis. Image Underst.* **77** (2000) 175 – 91
2. Benameur, S., Mignotte, M., Parent, S., Labelle, H., Skalli, W., de Guise, J.: 3D/2D registration and segmentation of scoliotic vertebrae using statistical models. *Computerized Medical Imaging and Graphics* **27** (2003) 321–37
3. Pennec, X.: Intrinsic statistics on Riemannian manifolds: Basic tools for geometric measurements. *Journal of Mathematical Imaging and Vision* (2006)
4. Fletcher, P., Lu, C., Pizer, S., Joshi, S.: Principal geodesic analysis for the study of nonlinear statistics of shape. *IEEE Trans. Med. Imaging* **23** (2004)
5. Boisvert, J., Pennec, X., Ayache, N., Labelle, H., Cheriet, F.: 3D anatomical variability assessment of the scoliotic spine using statistics on lie groups. In: *Proceedings of ISBI*. (2006)
6. Bergeron, C., Cheriet, F., Ronsky, J., Zernicke, R., Labelle, H.: Prediction of anterior scoliotic spinal curve from trunk surface using support vector regression. *Engineering Applications of Artificial Intelligence* **18** (2005) 973 – 82
7. Gonzalez, J., Varona, J., Roca, F., Villanueva, J.: Analysis of human walking based on aspaces. *Proc. of Articulated Motion and Deformable Objects* (2004) 177 – 88
8. Jiang, X., Motai, Y.: Learning by observation of robotic tasks using on-line pca-based eigen behavior. *Proc. International Symposium on Computational Intelligence in Robotics and Automation* (2005) 391 – 6
9. Pennec, X.: Computing the mean of geometric features - application to the mean rotation. *Research Report RR-3371, INRIA* (1998)
10. Aubin, C.E., Dansereau, J., Parent, F., Labelle, H., de Guise, J.: Morphometric evaluations of personalised 3d reconstructions and geometric models of the human spine. *Med. Bio. Eng. Comp.* **35** (1997)
11. King, H.A.: Selection of fusion levels for posterior instrumentation and fusion in idiopathic scoliosis. *Orthop Clin North Am* **19** (1988) 247–255
12. Little, J., Hill, D., Hawkes, D.: Deformations incorporating rigid structures. *Computer Vision and Image Understanding* **66** (1997) 223–32
13. Stokes, I.A., Spence, H., Aronsson, D.D., Kilmer, N.: Mechanical modulation of vertebral body growth. implications for scoliosis progression. *Spine* **21** (1996) 1162–1167